LEW-18738-1

Proceedings of ASME Turbo Expo 2010: Power for Land, Sea and Air
GT2010
June 14–18, 2010, Glasgow, UK

GT2010–22851

MODELING OF ATMOSPHERIC TURBULENCE AS DISTURBANCES FOR CONTROL DESIGN AND EVALUATION OF HIGH SPEED PROPULSION SYSTEMS

George Kopasakis
National Aeronautics and Space Administration
Glenn Research Center
Cleveland, Ohio 44135 USA

ABSTRACT

Atmospheric turbulence models are necessary for the design of both inlet/engine and flight controls, as well as for studying integrated couplings between the propulsion and the vehicle structural dynamics for supersonic vehicles. Models based on the Kolmogorov spectrum have been previously utilized to model atmospheric turbulence. In this paper, a more accurate model is developed in its representative fractional order form, typical of atmospheric disturbances. This is accomplished by first scaling the Kolmogorov spectral to convert them into finite energy von Karman forms. Then a generalized formulation is developed in frequency domain for these scale models that approximates the fractional order with the products of first order transfer functions. Given the parameters describing the conditions of atmospheric disturbances and utilizing the derived formulations, the objective is to directly compute the transfer functions that describe these disturbances for acoustic velocity, temperature, pressure and density. Utilizing these computed transfer functions and choosing the disturbance frequencies of interest, time domain simulations of these representative atmospheric turbulences can be developed. These disturbance representations are then used to first develop considerations for disturbance rejection specifications for the design of the propulsion control system, and then to evaluate the closed-loop performance.

NOMENCLATURE

a	speed of sound, (m/sec)
a_o	ambient speed of sound, (m/sec)
C_t	equivalent electric circuit capacitance for t-type of disturbance, (farads)
f	frequency, (Hz)
f_c	frequency of computed correction factor, (Hz)
h	altitude, (km)
k	wavenumber, (rad/m) or (cycles/m)
K_t	von Karman horizontal asymptote for t-type of disturbance
$K_{\omega n}$	adjustment factor to disturbance natural frequency
l	length, (m)
L	integral length scale, (m)
L_o	outer scale length, (m)
M	mach number
P	pressure, (Pa)
P_o	standard atmospheric pressure, (Pa)
q	fractional order of equivalent electrical circuit
R	universal gas constant, 287 (N*m)/(kg*K)
r	units conversion exponent of atmospheric disturbance
R_t	equivalent electric circuit resistance for t-type of disturbance, (ohms)
S	atmospheric turbulence spectral density
S_l, S_v	atmospheric velocity turbulence spectral density, $(m^3/sec^2)/(rad)$ or $(m/sec)^3/(Hz)$ also converted to (m/sec)/(Hz) by taking 1/3 root
S_T	temperature spectral density, $(K^2*m/s)/Hz$, also converted to $(K*(m/s)^{1/2})/Hz$
S_P	pressure spectral density, $(Pa^2*m/s)/Hz$, also converted to $(P*(m/s)^{1/2})/Hz$
s	Laplace operator
T	temperature, (K)
T_o	standard atmospheric temperature, (K)
v	flow velocity, (m/sec)
W	unity disturbance time domain signal
W_t	disturbance time domain signal for t-type of disturbance
x	fractional order of atmospheric disturbance spectral

Greek

α	constant associated with atmospheric turbulence spectral density α_l unit less, α_v unit less, α_T ($^oK^2sec^2m^{-2}$), and α_P ($Pa^2sec^2m^{-2}$)
γ	ratio of specific heats, ($\gamma = 1.41$)
ε	eddy dissipation rate, (m^2/sec^3)
η	the ratio of each decade interval where a pole or a zero will be used to estimate the fractional order TF

Copyright © 2010 by ASME

λ	wave length of atmospheric disturbance (m/cycle)
ρ	weight density, (kg/m^3)
ρ_{pz}	density of pole-zero pairs per decade for estimated TF
ω_f	natural frequency, (rad/sec)
ω_{pi}	frequency of TF pole *i* of whole order approx.(rad/sec)
ω_{zi}	frequency of TF zero *i* of whole order approx.(rad/sec)

Subscripts

a	constant associated with circuit capacitance correctional factor
A	variable associated with an adjustment
C	constant associated with circuit capacitance correctional factor
H	associated with symmetry frequencies for the approx.
fit	variable associated with TF fit or approximation
l	variable associated with longitudinal atmospheric disturbance
P	variable associated with pressure disturbance
t	variable associated with type of disturbance
T	variable associated with temperature disturbance
v	variable associated with vertical or transverse atmospheric disturbance
VK	variable associated with the von Karman spectral density
VKA	variable associated with the von Karman spectral density circuit approximation
o	variable associated with an output
p	variable associated with TF poles
s	variable associated with a static quantity
z	variable associated with TF zeros

INTRODUCTION

In this paper, atmospheric disturbance models are developed in both the time and the frequency domain. These models are applicable to propulsion system external flow field type disturbances that could also be extended to simulate vehicle gust loads. Furthermore, the models are valid over a wide range of altitudes and variations in atmospheric turbulence conditions. The objectives are as follows. First, develop computational models that are representative of the fractional order nature of actual atmospheric turbulence. Second, to employ these atmospheric models in the controller design process for supersonic vehicle air breathing propulsion system as an example. Finally, to develop specification considerations for supersonic vehicle atmospheric disturbances to be used for control design.

Atmospheric turbulence has been studied for some time, especially in the field of Atmospheric Sciences, Nastrom [1], and Fairall [2], and models have been developed. These models are primarily based on the so called Kolmogorov spectrum that was originally developed by Tararski [3], based partly on studies of turbulence by the Russian mathematician Andrei Kolmogorov [4-5]. The energy of the Kolmogorov spectrum asymptotically approaches infinity as frequency approaches zero, which makes it difficult to convert these types of models into time domain. The von Karman type model originally referred to as the isotropic-turbulence spectrum, Houbolt [6], is a commonly utilized atmospheric turbulence model approximation of the Kolmogorov disturbance with finite energy. However, simulating these types of models in time domain is problematic because of their fractional order.

The Kolmogorov model has also been extended by Tank [7] to develop a baseline of atmospheric turbulence for the High Speed Civil Transport (HSCT). The Tank model also covers atmospheric acoustic wave disturbance modeling using the von Karman spectral. Hoblit [8], introduced the Dryden model approximation to the fractional order von Karman atmospheric model. However, this model is a simplified second order approximation compared to the 5/3 fractional order of the acoustic velocity disturbance spectral. Thus, the Dryden model underestimates the atmospheric disturbances, increasingly with frequency.

To alleviate some of these difficulties, the Tank model for the von Karman approximation was utilized by Kopasakis [9] to derive an explicit electrical circuit analog of atmospheric disturbances. The circuit analog acts as a low pass filter where the circuit elements are explicitly computed as functions of atmospheric parameters, such as eddy dissipation rate and integral length scale. However, the circuit approximation also turns out to be fractional order, which makes it difficult to simulate. Thus, the circuit model was used by Kopasakis [9] to derive an integer order transfer function (TF) approximations to the fractional model with respect to the parameters describing atmospheric disturbances.

Fairall [2], Tank [7,10] and others approach atmospheric disturbance modeling probabilistically, as an *exceedance* for controls design purposes. That means that the probability of a time to failure is computed for controls design, such as inlet unstarts. This time to failure is associated with a controls design that can tolerate a maximum specified disturbance, and computes the probability, in terms of flight miles or hours, that an atmospheric disturbance will exceed this threshold. In this paper the approach will be to compute the expected worst case disturbance and assume that the control system will be designed to handle this disturbance. Thus, this development will not cover *exceedance rates*, which can be computed separately if desirable, based on the worst disturbances expected and the specifics of the controls design.

This paper is organized as follows. First, the Kolmogorov form of the atmospheric disturbance spectrum is presented, followed by the Tank model for the von Karman spectrum forms. Next the formulations that are used to approximate the fractional order atmospheric disturbance model using integer order TFs are presented. This is followed by providing considerations for atmospheric disturbance specifications for supersonic vehicle propulsion controls design. Finally, an example is presented for a supersonic inlet shock positioning feedback control design that employs these atmospheric disturbance formulations, followed by concluding remarks.

KOLMOGOROV FORM OF THE ATMOSPHERIC DISTURBANCE MODEL

Tank [7,10] utilized a Kolmogorov one-dimensional locally isotropic atmospheric turbulence spectrum, mathematically developed in Tararski [3], which represents the spectral density (in m^3/sec^2) for a structured random field of atmospheric turbulence as

Copyright © 2010 by ASME

$$S_t(k) = \alpha_t \varepsilon^{2/3} k^{-5/3} \tag{1}$$

The eddy dissipation rate, ε, in units of (energy/(mass × time)) = (m^2/sec^3), signifies the rate by which an atmospheric turbulence patch that reaches a critical Reynolds number successively dissipates to smaller and smaller turbulence structures, until it completely dissipates, Tararski [3]. The wave number k is in (cycles/m), Tararski [3], or in (rad/m), Tank [7,10]. For the Tank representation, the 2π factor used for the units conversion is absorbed into the α_t constants. Correspondingly, the spectral density of the acoustic wave velocity disturbance, $S_{l,v}(k)$, has units either in $((m/sec)^2/(rad/m))$ or $((m/sec)^2/(cycle/m))$. In this development more convenient units will be used of (m/sec) /Hz), by substituting *cycles* with Hz*sec and taking the 1/3 root.

The eddy dissipation rate varies significantly with altitude, especially at lower altitudes where atmospheric turbulences can become more severe, Fairall [2] and McMinn [11]. It also varies globally, Nastrom [1]. Tank [7] used a worst case value of $\varepsilon = 8.6\times10^{-5}$ based on data collected at altitudes ranging from 25 to 40,000 ft, which is about four times the appropriate value of ε for North Atlantic cruise altitudes. McMinn [11] derived ε values based on altitude and turbulence severity, using the Dryden turbulence parameters, Johnson [12], which show much greater values of ε, for severe turbulence. For supersonic cruise altitude, around 60,000 ft, the same value of ε can be used (for the same turbulence intensity), as ε stays about constant at these higher altitudes, above 20,000 ft.

The constant α_t is constant for each type of disturbance, given by Tank [7] to fit observed data:

- α_l = 0.15 (longitudinal (direction of flight) wind velocity gust, dimensionless)
- α_v = 0.2 (vertical or horizontal wind velocity gust, dimensionless)
- α_T = 0.39 (temperature disturbance, $°K^2s^2m^{-2}$)
- $\alpha_P = 5\times10^{-4}(P/T)^2$ (pressure disturbance, $Pa^2s^2m^{-2}$), where P and T are in total atmospheric quantities.

For a flight vehicle encountering an atmospheric disturbance with a wavenumber k in (cycles/m), the disturbance frequency experienced by the vehicle will be

$$f = \frac{Ma}{\lambda} = kMa \tag{2}$$

The speed of sound is related with temperature as

$$a = \sqrt{\gamma R T_s} \tag{3}$$

where T_s is the static temperature in °K, varying with altitude.

Figure 1 shows the zonal (east-west) winds, meridional (north-south) wind, and potential temperature power spectral as reported by Nastrom [1]. The units of the wind power spectral are in (m^3/sec^2)/rad and temperature is in ($°K^2m$/rad). As shown in Fig. 1, at wavelengths longer than 400 km, the power of turbulence decreases as the –3 power. For wavelengths below 400 km, the power of turbulence decreases as the –5/3 power

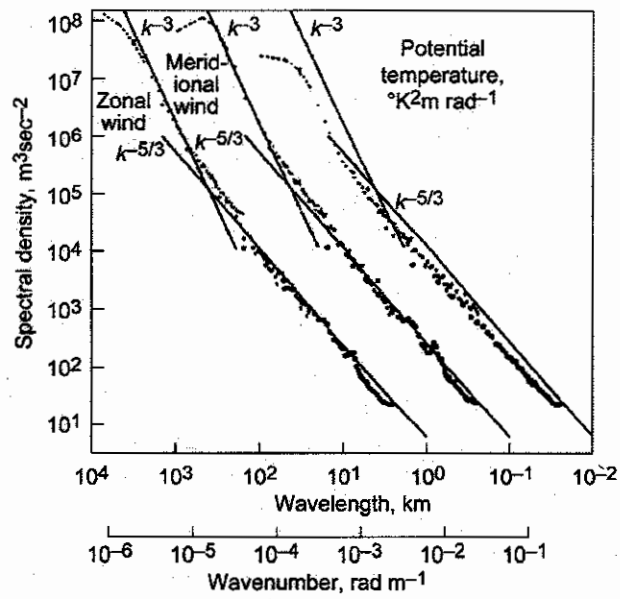

Figure 1.—Wind and Potential Temperature Spectra as reported by Nastrom [1]. Note: for clarity, the meridional wind and temperature spectra have been shifted one and two decades to the right, respectively.

which agrees with Eq. (1). Therefore, Eq. (1) is representative of atmospheric spectral density of disturbances when the wavelength is shorter than 400 km.

THE TANK MODEL

As an alternative to the Kolmogorov spectrum, Tank [10] and Soreide and Tank [13] scaled the von Karman spectrum to fit the Kolmogorov model in the limit (i.e., for large k), which compares well with other data and modeling efforts. For longitudinal disturbances this spectrum in (m^3/sec^2) is

$$S_{l,VK}(k) = 2.7\varepsilon^{2/3} L^{5/3} \frac{2}{\left[1+(1.339(2\pi)Lk)^2\right]^{5/6}} \tag{4}$$

For transverse disturbances, this spectrum is

$$S_{v,VK}(k) = 2.7\varepsilon^{2/3} L^{5/3} \frac{1+\frac{8}{3}(1.339(2\pi)Lk)^2}{\left[1+(1.339(2\pi)Lk)^2\right]^{11/6}} \tag{5}$$

The main difference of this von Karman form (compared to Kolmogorov model) is that the disturbance spectral levels off at low frequencies. Another difference is that the integral scale length, L, is explicitly stated in Eqs. (4) to (5). The integral scale length L is related to the outer scale length, L_o (the length of the atmospheric turbulence patch) by $L = L_o/14.7$ for the longitudinal disturbance, and $L = 2L_o/19$ for the transverse disturbance [13]. Figure 2 shows a plot of the Kolmogorov acoustic wave velocity spectral in (m/sec/Hz) using Eq. (1), compared to the corresponding von Karman spectral for the longitudinal and transverse acoustic wave velocity

Copyright © 2010 by ASME

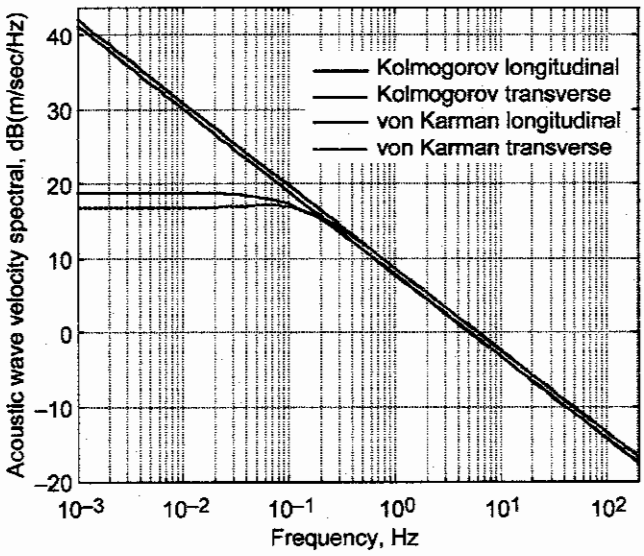

Figure 2.—Acoustic wave velocity spectral comparisons for the Kolmogorov and von Karman spectral.

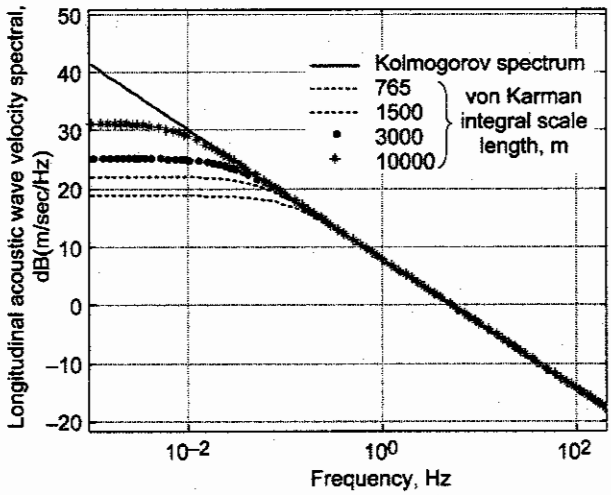

Figure 3.—Longitudinal acoustic wave velocity spectral comparisons for different integral length scales.

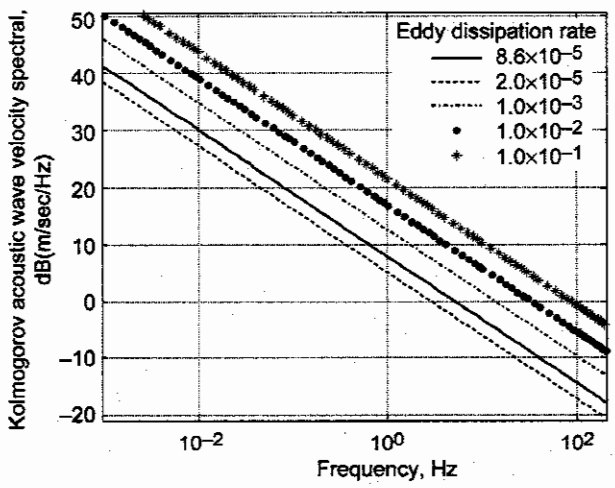

Figure 4.—Longitudinal acoustic wave velocity spectral comparisons for different eddy dissipation rates.

disturbances, Eqs. (4) to (5). Different values of L will produce the same curves with either higher or lower low-frequency asymptote as shown in Fig. 3 for the longitudinal disturbance. Soreide & Tank [11] used a value of L=762 m, which they called as standard in the airplane industry. Since a typical control design is expected to sufficiently attenuate disturbances at frequencies well beyond 1 Hz, based on Fig. 3 differences in the value of L (i.e., differences in the lower frequency asymptote) will have negligible effect on the control system performance. The Kolmogorov spectrum for the longitudinal acoustic wave velocity is also shown in Fig. 4 with different values of eddy dissipation rates. As noted from this figure, orders of magnitude difference in the eddy dissipation rate don't produce as appreciable change in the Kolmogorov spectral density. For instance, approximately four orders difference in ε only makes approximately a factor of 8 differences in velocity as

$$S_1(f) = \left(\frac{\varepsilon_1}{\varepsilon_2}\right)^{2/9} S_2(f) \tag{6}$$

FRACTIONAL ORDER FIT OF ATMOSPHERIC TURBULENCE MODEL

Atmospheric turbulence, as shown in Fig. 1 and as described by Kolmogorov and the Tank models in Eq. (1) and Eqs. (4) to (5), is fractional order. Kopasakis [9] utilized a circuit analog of the von Karman form of the Tank model, which serves as the basis for deriving integer order pole-zero product TF approximations to the fractional order atmospheric disturbances. The reason for the need to derive approximations to the fractional order equations is because of the difficulty of explicitly or numerically solving fractional order differential equations.

The idea behind the integer order TF approximation to a fractional order TF is as follows: Starting somewhere near the beginning of the equivalent 3 dB frequency of the fractional order TF, a whole order TF approximation can be developed symmetrically centered around the fractional order TF, like a descending staircase shape, by interleafing integer order poles and zeros. As the number of steps of this staircase TF approximation increase, the steps become shorter, eventually collapsing to the straight line of the fractional order TF as the number of poles and zeros of this approximation is increased to infinity. For this to work, the frequency of the poles and zeros need to (a) be related to the atmospheric disturbance parameters and (b) the location of these frequencies need to be derived in a way such that the staircase TF approximation is symmetrically centered around the fractional order TF.

The fractional order circuit analog of Eqs. (4) to (5) is shown in Fig. 5. Based on this analog, see Ref. [9] for detailed derivations, the capacitance of the circuit can be derived as

$$C_t = \frac{1}{\left(a_t \varepsilon^{2/3}\right)^{1/x} (2\pi Ma)} \tag{7}$$

and the resistance can be derived as

$$R_t = 1.339(2\pi)\left(a_t \varepsilon^{2/3}\right)^{1/x} L \tag{8}$$

Copyright © 2010 by ASME

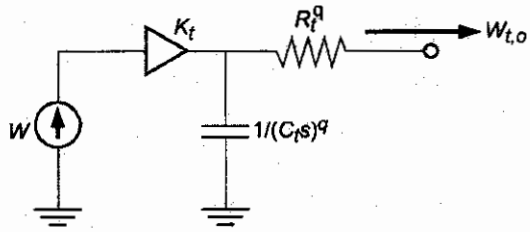

Figure 5.—Equivalent TF of atmospheric disturbance.

The natural frequency of this circuit is

$$\omega_f = \frac{K_{\omega n}}{R_t C_t} \tag{9}$$

Where the adjustment factor $K_{\omega n}$ is 1 for this circuit, but represented in this form in case any adjustments need to be made to the atmospheric disturbance natural frequency.

Based on these circuit analog parameters, a time domain disturbance can be derived based on an integer order TF approximation for atmospheric turbulences, given the atmospheric disturbance parameters ε, L, q, t, and r for the units conversion factor (with q=xr; x=5/3 and r=1/3 for acoustic disturbances and ½ for temperature and pressure) as

$$W_{t,o} \cong K_{t,fit} \frac{\prod_{1}^{m_z}(s/\omega_{zi}+1)}{\prod_{1}^{m_p}(s/\omega_{pi}+1)} W_t \tag{10}$$

where W_t is series of sinusoids with unit amplitude frequency components distributed over the frequency range of interest. The frequencies of the poles can be computed as

$$\omega_{pi} = \frac{K_{\omega pi}\omega_{Hpi}\prod_{j=1}^{i-1}(\omega_{Hpi}/\omega_{pi-j}+1)}{10^{\eta(2i-1)*q}\prod_{j=1}^{i-1}(\omega_{Hpi}/\omega_{zi-j}+1)-1} \quad i=2,3\ldots,m_p, \tag{11}$$

where the first pole is computed as follows

$$\omega_{p1} = \omega_f\left(10^{\eta q}-1\right)^{\frac{1-q}{q}} \tag{12}$$

and the frequencies of the zeros can be computed as

$$\omega_{zi} = \frac{K_{\omega zi}\omega_{Hzi}\prod_{j=1}^{i-1}(\omega_{Hzi}/\omega_{zi-j}+1)}{10^{-2\eta i*q}\prod_{j=1}^{i}(\omega_{Hzi}/\omega_{pi}+1)-1} \quad i-1,2\ldots m_z, \tag{13}$$

Thus, for n number of frequency decades desired to be estimated

$$m_p = (n-1)/\eta \tag{14}$$

$$m_z = m_p - 1 \tag{15}$$

For a desirable polo-zero density pair, ρ_{pz}, per decade to be used to approximate the fractional order disturbance

$$\eta = \frac{1}{2\rho_{pz}} \tag{16}$$

and ω_{Hpi}, ω_{Hzi} in Eqs. (11) to (12) can be computed as

$$\omega_{H_{pi}} = \omega_f(10^{\eta q(2i-1)}-1)^{1/q}, \quad i=2\ldots,m_p, \tag{17}$$

$$\omega_{H_{zi}} = \omega_f(10^{2\eta qi}-1)^{1/q}, \quad i=1,2\ldots,m_z, \tag{18}$$

The utility of ω_{Hpi} and ω_{Hzi} are to maintain symmetry, so that the staircase pole-zero approximation is symmetrically located on top of the fractional order TF asymptote. The proportional gains $K_{\omega pi}$ and $K_{\omega zi}$ in Eqs. (11) to (12) are reserved for final adjustments that may be needed to these frequencies for more closely approximating the fractional order TFs representing atmospheric disturbances.

Longitudinal and Transverse Acoustic Wave Turbulence

The longitudinal and transverse acoustic wave atmospheric disturbances are in the form of pure wind gusts in the axial direction of vehicle motion for the longitudinal disturbance, and in the vertical direction of motion for the transverse disturbance. Based on the fractional order fits performed by Kopasakis [9], using Eqs. (7) to (17), with q=xr=5/9 (r=1/3), then $K_{t,fit}$ in Eq. (10), based on inspection of Eqs. (4) to (5), is

$$K_{l,fit} = \left(5.4\varepsilon^{2/3}L^{5/3}\right)^{1/3} \tag{19}$$

for the longitudinal disturbance, and

$$K_{v,fit} = \left(2.7\varepsilon^{2/3}L^{5/3}\right)^{1/3} \tag{20}$$

for the transverse disturbance. For n=3 (i.e., the TF fit over the span of 3 decades in frequency), the proportionality factor adjustments to improve these fits have been found to be [9],

$$K_{l,\omega} = \left[K_{\omega n}, K_{\omega pi}, K_{\omega zi}\right] = [2.4; 1\ 1\ 1/2.4\ 1/1.5; 1\ 1\ 1] \tag{21}$$

for the longitudinal acoustic wave, and

$$K_{v,\omega} = \left[K_{\omega n}, K_{\omega pi}, K_{\omega zi}\right] = [4.27; 1\ 1\ 1/2.4\ 1/1.5; 1\ 1\ 1] \tag{22}$$

for the transverse. These TF fits compared to the von Karman spectral using the Tank model Eqs. (4) to (5) with the units conversion exponent r, are shown in Figs. 6 to 7, for ε=8.5×10^{-5} (m^2/sec^3) and L=762 m. As shown in these figures, the fits do a good job in approximating these disturbances. More accuracy can be achieved around the knee of these spectral by increasing the density of pole-zero pairs per frequency decade in this region.

Copyright © 2010 by ASME

A certain inaccuracy at such low frequency would be acceptable for a feedback control design, since a typical control design should have no problem attenuating low frequency disturbances.

Temperature Turbulence

Atmospheric temperature turbulence causes both temperature as well as acoustic velocity disturbances due to the change in the speed of sound. For the most part temperature disturbances result in vertical displacement of air parcels (so called gravity waves). Therefore, acoustic velocity disturbances caused by temperature will generate vertical wind gusts that add with any transverse acoustic velocity gusts. However, for the propulsion system, according to Ashun, [14], the wing forebody will turn a vertical gust into a longitudinal gust, by multiplying the vertical gust by the conversion factor $(M_\infty - 1)/\sqrt{M_\infty^2 - 1}$, which amounts to 0.63 for M_∞ =2.35. In subsequent discussion, this factor will not be used since for worst case purposes this conversion correction factor is not deemed significant.

In Ref. [9], first the Kolmogorov spectrum of the longitudinal acoustic wave and that of the temperature, based on Eq. (1), are plotted. This results in parallel spectral lines with frequency, similar to the Kolmogorov spectra shown in Fig. 2. Then the von Karman temperature spectral is constructed by scaling the horizontal von Karman type acoustic wave spectral (i.e., scaling it by the difference in magnitudes of these Kolmogorov spectra).

Temperature turbulence, as can be seen in Fig. 1, also follows the 5/3 law, but its units are in terms of Kelvin squared. Thus, in order to convert the units to Kelvin, the exponent r becomes ½, which makes the fractional order q=5/6. Based on this, the TF fit performed for temperature in Ref. [9] was done the same way as with acoustic wave in the previous section (i.e., utilizing Eqs. (7) to (18), with the additional relations.

$$K_{T,fit(temp)} = \sqrt{14.0\varepsilon^{2/3}L^{5/3}} \tag{23}$$

$$K_{T,\omega} = [K_{\omega n}, K_{\omega pi}, K_{\omega zi}] = [1.5; 1\ 1\ 1/1.1\ 1/1.2; 1\ 1\ 1] \tag{24}$$

Figure 8 shows this TF fit and the spectral of Eq. (4) (i.e., Eq. (4) scaled using Eq. (23) and by also applying the units conversion factor in the denominator). Once a particular fit is performed (i.e., acoustic wave velocity, temperature, pressure or density), the proportional factors (such as Eqs. (21), (22), and (24)) do not need to be recomputed for different atmospheric turbulence parameter values.

By perturbing the relation of the speed of sound and temperature in Eq. (3), and substituting the resulting expression for Δa into the Mach number equation of $M=v/a$, the relation between the change in temperature and acoustic velocity can be obtained as

$$\Delta v = \frac{M\gamma R}{2a_o}\Delta T \tag{25}$$

Based on this relation between temperature variations and acoustic velocity, then $K_{T,fit(acoustic)}$ for the acoustic wave velocity

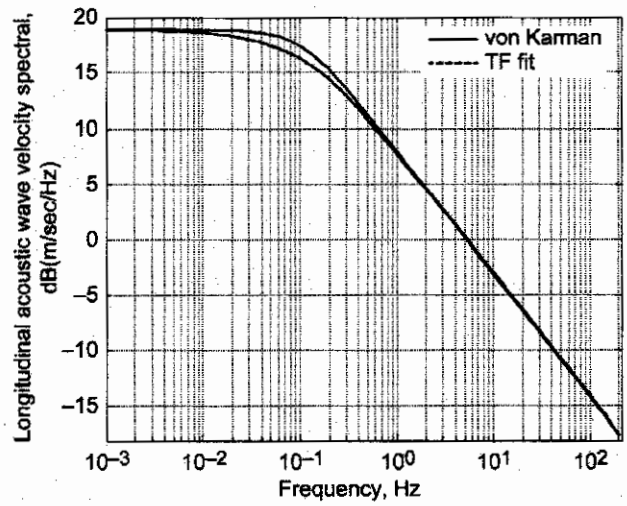

Figure 6.—Longitudinal von Karman spectral, final adjusted TF fit.

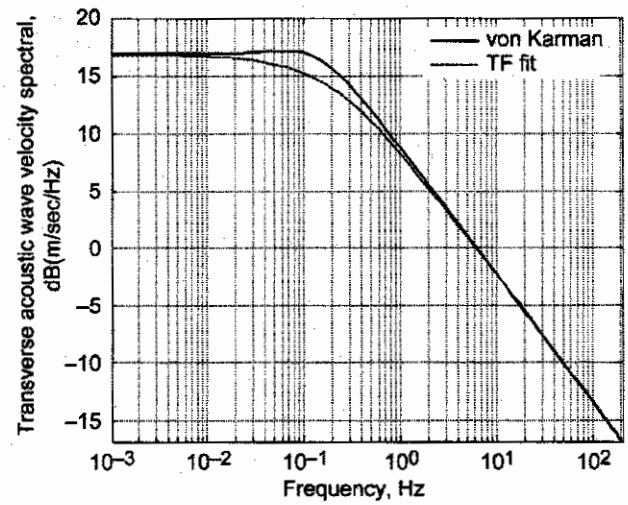

Figure 7.—Transverse von Karman spectral, final adjusted TF fit.

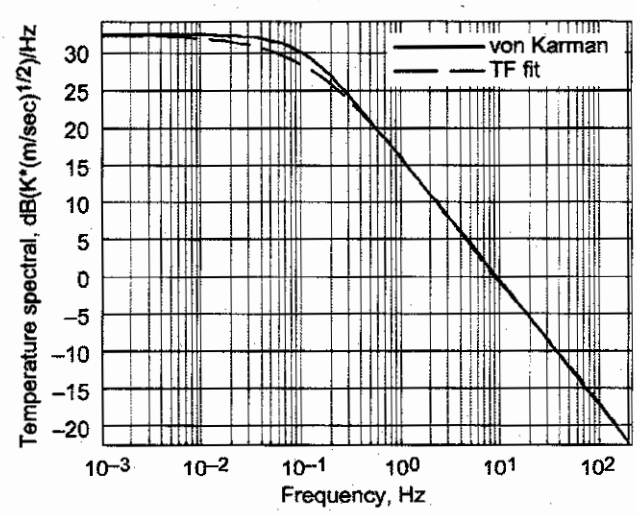

Figure 8.—Temperature von Karman spectral and its TF fit.

Copyright © 2010 by ASME

disturbance due to an atmospheric temperature fluctuation can be computed as

$$K_{T,fit(acoustic)} = \frac{M\gamma R}{2a_o}\sqrt{14.0\varepsilon^{2/3}L^{5/3}} \tag{26}$$

The proportionality factors of Eq. (24) remain the same for the acoustic wave TF fit due to temperature fluctuations. This TF fit for the acoustic velocity disturbance at supersonic cruise altitude, at Mach 2.35, for L=762 m and two different values of ε is shown in Fig. 9. The TF fit for $\varepsilon=8.5\times10^{-5}$ (m^2/sec^3) and for two different values of integral scale lengths is shown in Fig. 10. As can be seen from this figures, the acoustic velocity gusts produced by fluctuations in temperature are much higher in amplitude than those produced by pure acoustic velocity gusts.

Pressure Turbulence

The longitudinal velocity wave spectral and the pressure spectral of Eq. (1) was utilized the same way as described in the previous section for the temperature to scale the von Karman type acoustic wave spectral to come up with the pressure spectral of atmospheric disturbances, [9]. The units conversion exponent for pressure is the same as that for temperature (i.e., r=1/2), which makes the fractional order the same (i.e., q=5/6). As such, $K_{p,fit}$ and $K_{p,\omega}$ were computed as follows, [9]

$$K_{P,fit} = \sqrt{11.6\varepsilon^{2/3}L^{5/3}} \tag{27}$$

$$K_{P,\omega} = \left[K_{\omega n}, K_{\omega pi}, K_{\omega zi}\right] = \left[1.5; 1\ 1\ 1/1.1\ 1/1.2; 1\ 1\ 1\right] \tag{28}$$

Figure 11 shows this TF fit for $\varepsilon=8.5\times10^{-5}$ (m^2/sec^3) and L=762 m compared to the scaled von Karman type spectral (i.e., Eq. (27) substituted for the numerator and proportional factor of Eq. (4) with the denominator of Eq. (4), raised to the power r).

Density Turbulence

Density disturbances are contained within temperature and pressure fluctuations and its inclusion in a simulation, along with pressure and temperature will produce unnecessarily additional disturbances. However, if need be, the relation of density disturbance with temperature and pressure can be derived as (by perturbing the state equation)

$$\Delta\rho = \frac{P_o + \Delta P}{R(T_o + \Delta T)} - \frac{P_o}{RT_o} \tag{29}$$

CONSIDERATIONS FOR ATMOSPHERIC TURBULANCE SPECIFICATIONS

As discussed in the introduction, the approach will be to compute the worst case disturbances expected, assuming that the control system can be designed to handle these disturbances. As will be discussed later, these worst case atmospheric disturbances would be assumed for light to moderate levels of turbulence. For severe turbulence, it would be assumed that some kind of schedule will be used for the shock reference position control so the performance of the propulsion system is not penalized under usual atmospheric conditions. Unlike earlier developments like Fairall [2], Tank

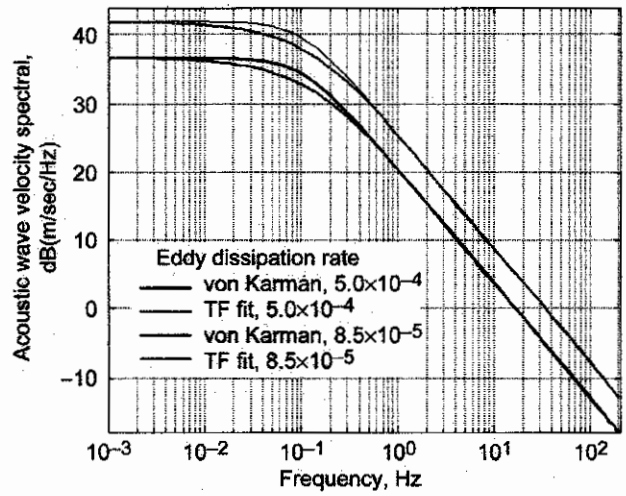

Figure 9.—von Karman acoustic wave velocity spectral due to temperature gust and its TF fits for different eddy dissipation rates.

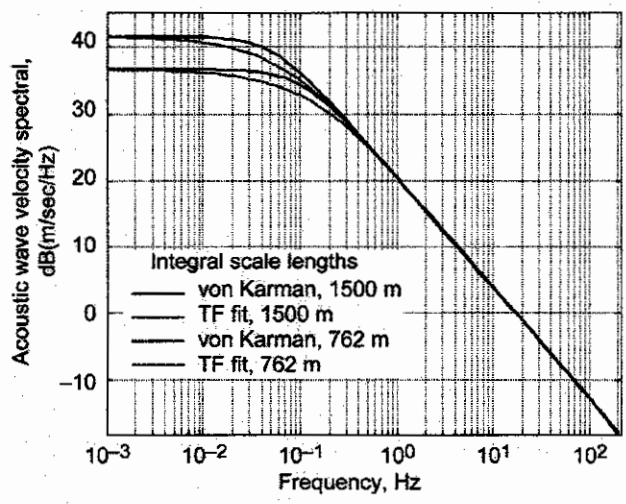

Figure 10.—von Karman acoustic wave velocity spectral due to temperature gust and its TF fits for different integral scale lengths.

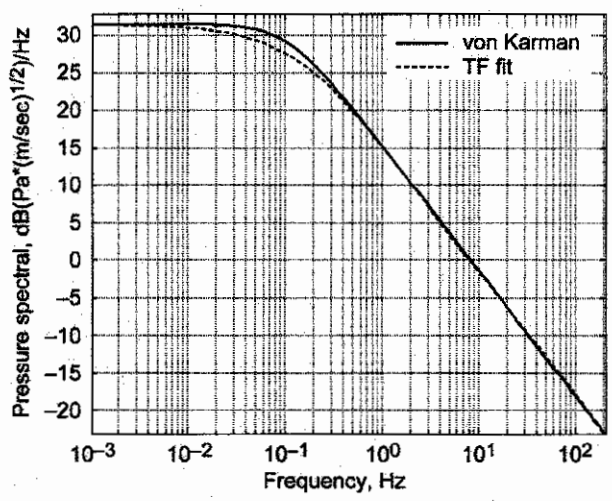

Figure 11.—Pressure von Karman spectral and its TF fit.

Copyright © 2010 by ASME

[7,15] and others, the approach here is to analyze the control design for worst case disturbances, and as such the analysis presented does not cover *exceedance rates*, which can be computed separately, if the need arises.

The TF fits derived in the previous sections can be thought of as filters, which take input disturbances represented by unit amplitude sinusoids of different frequencies and convert them to representative free stream atmospheric disturbances. Because the TF fits contain the representative magnitudes of these disturbances, the input time domain frequencies components of W_t only need to have unity RMS values.

As an input to these TFs representing atmospheric disturbances, a sum of unit amplitude sinusoids can be constructed in time domain, starting at some low frequency and continuing up to the frequencies of interest for the control system. The control design can also be verified for the disturbance attenuation it provides at specific frequencies, by simulating single frequency sinusoids. In addition, the control design can be verified against sinusoidal disturbances, clustered at specific frequency bands that simulate the vehicle Mach number frequency dependence as represented by Eq. (2). The disturbance frequencies that the vehicle sees, also depends on the smallest atmospheric turbulence dissipation scales, which will be discussed shortly. When a series of sinusoids are simulated to represent atmospheric disturbances, it is also assumed that the total magnitude of the disturbance, such as the magnitude of the acoustic velocity gust, should not exceed certain maximum specified amplitude.

The length of atmospheric turbulence patches can range from 100's km down to a few kilometers. A feedback control system will normally have the most difficulty attenuating the higher frequencies of these disturbances, as the bandwidths of control systems are limited. However, because the spectral densities of atmospheric disturbances drop off with frequency, see Figs. 6 to11, it can also turn out that the mid-frequency range of atmospheric disturbances becomes most challenging to the control system design.

From Eq. (2), for a supersonic vehicle flying at Mach 2.35 at an altitude of 18 km, encountering an atmospheric turbulence of 5 km long, the frequency of the disturbance will be around 0.14 Hz. As atmospheric disturbances dissipate, they do break into small scale disturbances, which can produce higher frequencies. For a shock control system with a 100 Hz bandwidth, which would be near the limits of what can be practically achieved with this type of control system design, the length of the small scale disturbance up to which the control system can provide attenuation is about 7 m long, Eq. (2). According to Fairall, [2], the smallest scale, under dissipation, to apply the spectral for gravity waves (associated with temperature disturbances) was calculated to be 50 m, and compromised to 25 m by factoring in estimations from other sources. For a smallest disturbance scale of 25 m or k=0.04 cycles/m and by taking into account the vehicle speed (i.e., M=2.35 in this case), then the highest disturbance frequency turns out to be f=28 Hz, which will normally be within the expected control bandwidth.

Thereby, for a vehicle cruising at Mach 2.35, the control system design with clustered atmospheric disturbance frequency components up to 28 Hz will also need to be considered. For lack of information, in terms of maximum wind velocities, maximum local wind velocities of 180 miles for high altitudes (starting at altitudes where the vehicle will be transitioning through the transonic regime) will be assumed. Even though light to moderate turbulence levels are considered under normal conditions for this design, the assumption is that smaller turbulence structures under dissipation can momentarily produce relatively high wind velocities.

It is also assumed here that a worst case atmospheric disturbance can include wind gusts from pure acoustic wave velocity gusts as well as wind gusts due to temperature fluctuations, together with temperature fluctuations, as well as pressure fluctuations. Temperature disturbances normally appear as gravity waves transverse disturbances, Fairall [2], converted to longitudinal gusts for the propulsion system via the vehicle wind forebody, Ashun [14]. As discussed earlier, different values of the integral length scale will not significantly affect the control system design, see Fig. 3. On the other hand, differences in the eddy dissipation rate, Fig. 4, will affect the controls design and a worst case value of 8.6×10^{5} was used by Soreide and Tank [13] for high altitudes (presumably for light to moderate turbulence). Compared with the assumption here of a combined worst case disturbance that includes wind gusts, temperature and pressure fluctuations at the same time, Soreide and Tank [13] assumed a worst case disturbance that only includes wind gust produced from pure acoustic velocity type disturbances.

According to McMinn [11], which provides an analysis table that shows how ε varies with altitude, at supersonic cruise altitude the value of ε varies between 2×10^{5}, 2×10^{-2}, and 1.3×10^{-1}, for light to moderate to severe turbulence, respectively. On the other hand, Tank [7], sites different references with recorded ε observations at high altitudes, which shows a maximum recorded ε of 1.7×10^{-3}. In any case, in order to deal with large variations in ε, and not to unnecessarily penalize the performance of the propulsion system in terms of inlet pressure recovery (which affects propulsion efficiency), it may become appropriate to incorporate sensors to detect higher levels of turbulence and to schedule the controlled shock reference position accordantly.

For a propulsion system controls design, like the case of shock positioning controls design for a supersonic vehicle, the assumption is that this worst case atmospheric disturbance will produce wind gusts in the longitudinal direction. That is in the direction of the vehicle flight path, and that a combined longitudinal and transverse disturbance will not produce worst conditions for the control system design as compared with that of the longitudinal gust alone. For studying the effects of inlet flow distortion on the propulsion system, the affects of the combined longitudinal and transverse disturbances may need to be considered.

PROPULSION CONTROLS DESIGN EXAMPLE UTILIZING ATMOSPERIC TURBULANCE

A feedback controls design example for shock position controls for an internal compression supersonic inlet is discussed in this section, where these atmospheric turbulences are utilized. More detail on this inlet controls design can be found in Kopasakis [16]. For some background, the shock

Copyright © 2010 by ASME

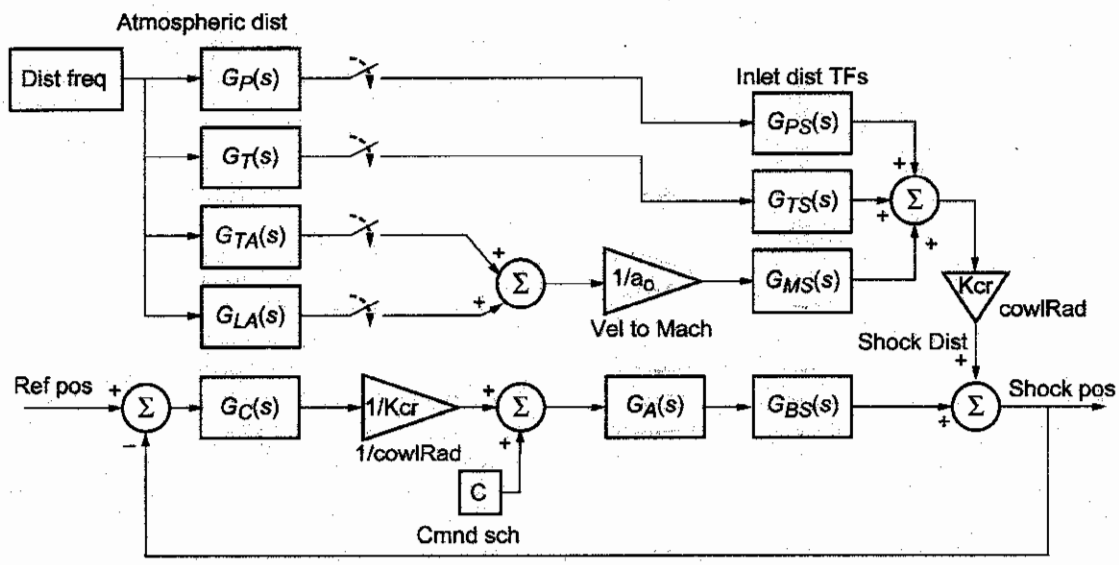

Figure 12.—Feedback control diagram of inlet shock position system via bypass door actuation.

position is controlled at a reference position downstream of the inlet throat. The closer the shock position is to the inlet throat, the higher is the inlet pressure recovery. For all practical purposes, if the shock reaches the minimum throat restriction, it quickly gets expelled from the inlet and the inlet unstarts, which is undesirable.

Figure 12 shows the feedback controls diagram for the supersonic inlet shock position controls design. For more detail on this design see Ref. [16]. In this diagram, G_c stands for the feedback controller TF; G_{BS} is the bypass door to shock position TF; G_A is the bypass door actuator TF which is simulated as a feedback system with its own controls; G_{PS}, G_{TS}, and G_{MS} are disturbance TF from upstream flow field disturbances to shock position; and finally G_P, G_T, G_{TA}, and G_{LA} are atmospheric disturbance TF for pressure, temperature, acoustic disturbance due to temperature, and the longitudinal acoustic disturbance respectively, all listed in Ref. [16]. Based on the derivations for the atmospheric disturbance TF carried out in the previous section, these TF can be calculated for L=765 and e=8.6×10^5 as

$$G_{LA}(s) = \frac{8.74(s/9.2+1)(s/55.0+1)(s/335.5+1)}{(s/1.46+1)(s/30.1+1)(s/85.7+1)(s/1593.1+1)} \quad (30)$$

$$G_T(s) = \frac{41.75(s/33.0+1)(s/45.6+1)(s/602.4+1)}{(s/1.1+1)(s/25.1+1)(s/109.8+1)(s/816.3+1)} \quad (31)$$

$$G_{TA}(s) = \frac{M\gamma R}{a_o}\frac{20.88(s/33.0+1)(s/45.6+1)(s/602.4+1)}{(s/1.1+1)(s/25.1+1)(s/109.8+1)(s/816.3+1)} \quad (32)$$

$$G_P(s) = \frac{37.96(s/33.0+1)(s/45.6+1)(s/602.4+1)}{(s/1.1+1)(s/25.1+1)(s/109.8+1)(s/816.3+1)} \quad (33)$$

The feedback controls design methodology utilized in Ref. [16] for shock position is based on the feedback control systems loop shaping design approach developed by Kopasakis [17], extended to multi-loop feedback control systems. In this approach, the closed loop gain for the control system is designed first, based on the actuator bandwidth and also maximizing the system performance, such as disturbance rejection and stability margins. Then, by also knowing the plant TF, the controller feedback TF is automatically calculated [16], and finally this TF is fitted with poles and zeros to derive the control law. Based on this approach, the controller TF calculated and fitted [16], is

$$\begin{aligned} G_C(s) = {} & \frac{100(s/2\pi5+1)(s/2\pi18.8+1)}{s(s/2\pi14.5+1)(s/2\pi104+1)} \\ & \frac{(s^2/(2\pi145)^2+0.98s/2\pi145+1)}{(s^2/(2\pi5000)^2+1.4s/2\pi5000+1))} \\ & \frac{(s^2/(2\pi250)^2+1.3s/2\pi250+1)}{(s^2/(2\pi5500)^2+1.4s/2\pi5500+1} \\ & \frac{(s^2/(2\pi350)^2+1.36s/2\pi350+1)}{(s^2/(2\pi6000)^2+1.4s/2\pi6000+1)} \\ & \frac{(s^2/(2\pi450)^2+1.0s/2\pi450+1)}{(s^2/(2\pi6500)^2+1.4s/2\pi6500+1)} \\ & \frac{(s^2/(2\pi550)^2+1.0s/2\pi550+1)}{(s^2/(2\pi7000)^2+1.4s/2\pi7000+1)} \\ & \frac{(s^2/(2\pi650)^2+0.60s/2\pi650+1)}{(s^2/(2\pi7500)^2+1.4s/2\pi7500+1)} \end{aligned} \quad (34)$$

A combined atmospheric disturbance consisting of a pure acoustic wave wind gust accompanied by a temperature fluctuation that also produces acoustic wave velocity disturbances, together with a pressure fluctuation was applied to the control system shown in Fig. 12, Ref. [16]. For this disturbance, Eqs. (30) to (33) were utilized with an input

Copyright © 2010 by ASME

consisting of 8 unit amplitude sinusoids distributed from very low frequencies up to 200 Hz. The various components of this disturbance (i.e., the acoustic frequency components of velocities, temperatures and pressures) are all in phase in this simulation, which will produce even worse conditions. A time domain slice of these disturbances is shown in Fig. 13, with worst case eddy dissipation rate of light to moderate turbulence of $\varepsilon=8.6\times10^5$. The number and frequencies of the input sinusoids chosen for this problem produce peak wind gusts of approximately 180 mph; approximately 80 m/sec (as discussed in the previous section), see Fig. 13. As seen in this figure, temperature fluctuations produce much more pronounced wind gust, than those due to pure acoustic wave disturbances. As discussed before, the range of values of εthat signify different levels of turbulence are also accompanied by peak wind gusts limits or specifications, when constructing time domain simulations. Normally, for low frequency disturbances, even if peak wind gust values are exceeded, this should not have that much impact on the controller response. However, higher frequencies will have an impact because the control system disturbance attenuation capability reduces with frequency. Thus, in this simulation the value chosen of $\varepsilon=8.6\times10^5$, is also accompanied by a peak wind gust value of approximately 180 mph, by assuming that dissipation of small scale turbulence structures can momentarily produce high values of wind gusts.

Figure 14 shows the shock position disturbance that the controller sees as a result of the atmospheric turbulence that is applied, the controller command, the valve position output command, and the controlled shock position response. As can be seen, the controller in this design keeps the shock position within a range of 0.15 in., which is very good. For instance, if such tight shock position control could be maintained for all expected inlet disturbances, it could improve the pressure recovery and therefore, the overall inlet propulsion efficiency. As described in the previous section, the highest disturbance frequency that the vehicle is expected to see is about 28 Hz. This is computed by taking into account the vehicle's supersonic speed and by also considering the smallest expected dissipative turbulence structures. In order to simulate clustered atmospheric components up to this frequency, a combined atmospheric disturbance was applied as before, but this time with 32 unit amplitude sinusoids distributed from 1 to 30 Hz. The combined acoustic velocity disturbance (i.e., the acoustic velocity due to a pure acoustic velocity gust and that

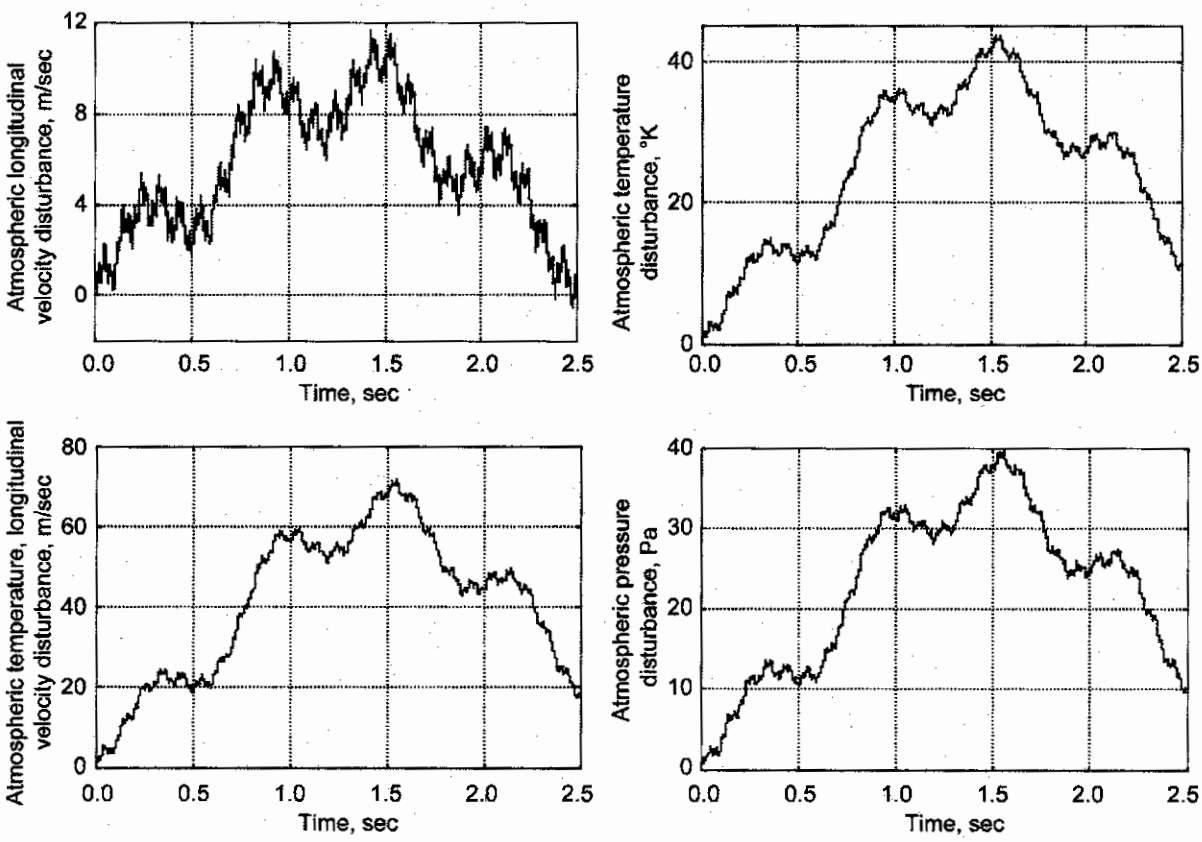

Figure 13.—Atmospheric disturbances of Eqs. (29) to (32), with unit amplitude input sinusoids.

Copyright © 2010 by ASME

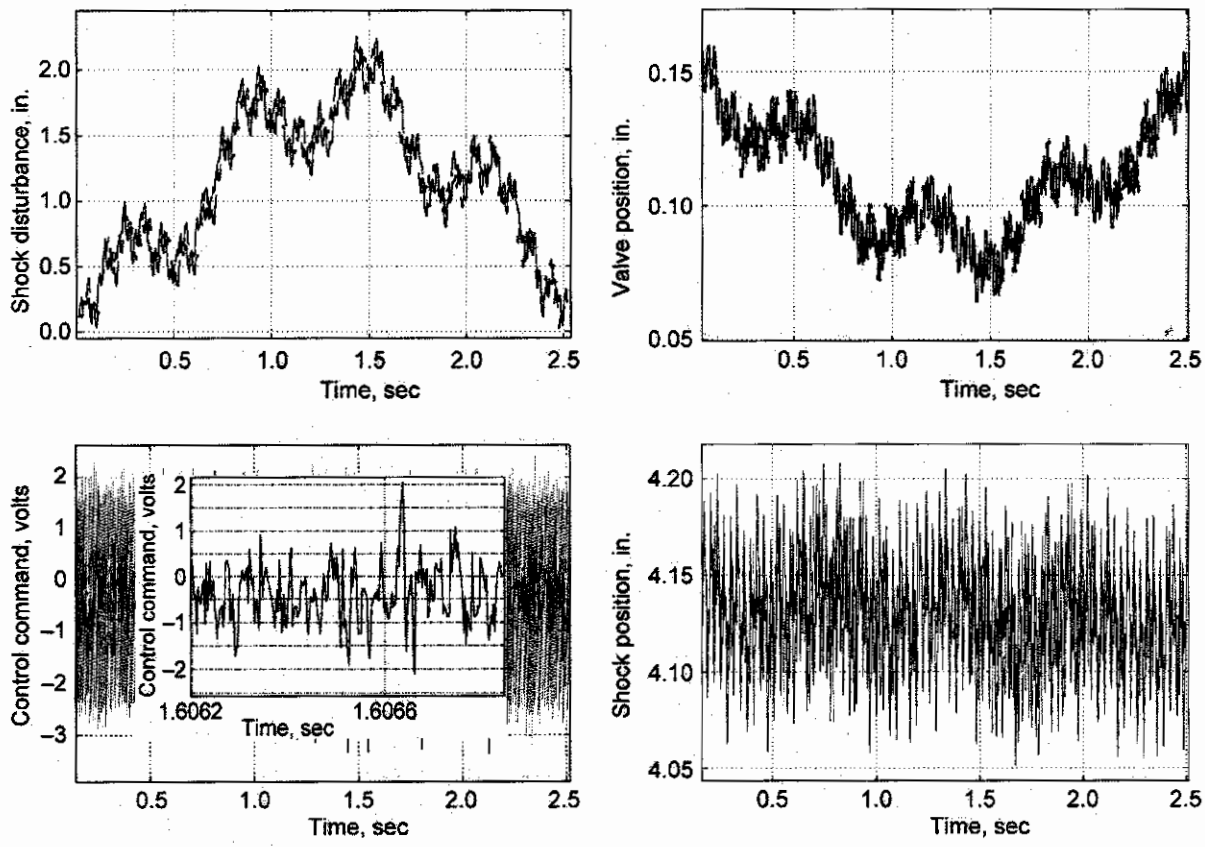

Figure 14.—Shock disturbance, control command, valve position, and shock position response due to atmospheric disturbances.

due to temperature fluctuation) is shown in Fig. 15. The shock position disturbance produced from this atmospheric disturbance is shown in Fig. 16, and the controlled shock position response is shown in Fig. 17. The shock position this time varies within approximately 0.4 in., compared to 0.15 in. in the simulation shown in Fig. 14. The reason is that the close proximity of the disturbance frequencies generates additional frequencies, which can be significantly higher in amplitude than those of the individual sinusoids alone. As seen in Fig. 15, at approximately 4 sec, the wind gusts well exceed 180 mph. However, there is little difference in the shock control response at 4 sec, Fig. 17, which indicates that for this simulation at this lower frequency range, the peak amplitude for wind gust is not a limiting factor for this control system.

Figure 18 shows a combined atmospheric disturbance distributed from 5 to 30 Hz at 1 Hz intervals, but with a higher eddy dissipation rate of $\varepsilon=1.7\times10^{-3}$, which is the highest measured ε as discussed in the previous section. The peak wind gusts generated from this disturbance, based on the sinusoids components selected for this disturbance, is in excess of 200 mph. The shock disturbance and the control response, due to this disturbance, are shown in Figs. 19 to 20 respectively. The peak-to-peak shock position varies within approximately 1 in. Thus, this serves as an example if the control system design would need to handle, under normal conditions, moderate turbulence [11], or highest recorded turbulence [7] as discussed before, with peak wind gust limits as shown here. It would however, be a question whether an actual atmospheric disturbance can exhibit such a behavior (i.e., such closely clustered sinusoids in a narrow frequency band).

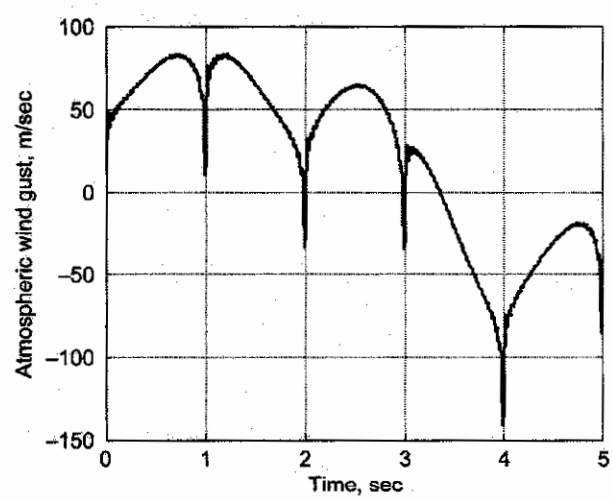

Figure 15.—Combined atmospheric wind gust for disturbance frequencies 0.2 to 30 Hz, with $\varepsilon = 8.6\times10^{-5}$.

Copyright © 2010 by ASME

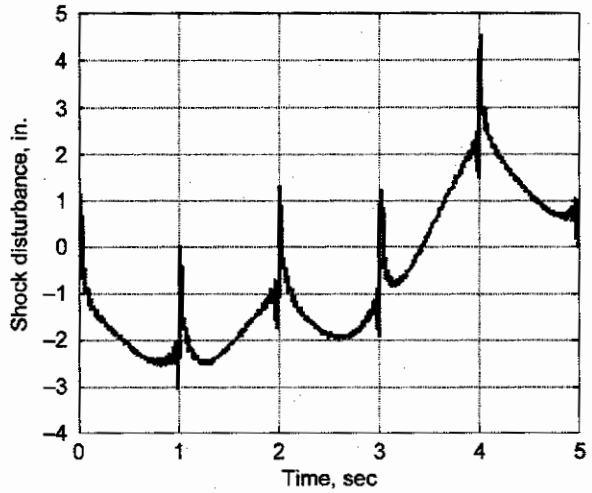

Figure 16.—Shock disturbance for disturbance frequencies 0.2 to 30 Hz, with $\varepsilon = 8.6\times10^{-5}$.

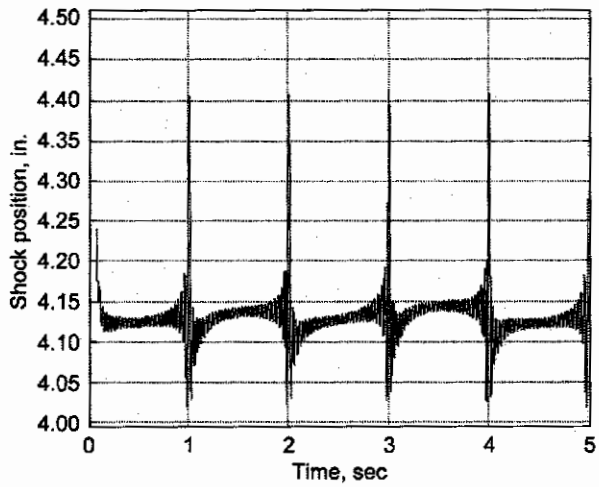

Figure 17.—Shock control response for disturbance frequencies 0.2 to 30 Hz, with $\varepsilon = 8.6\times10^{-5}$.

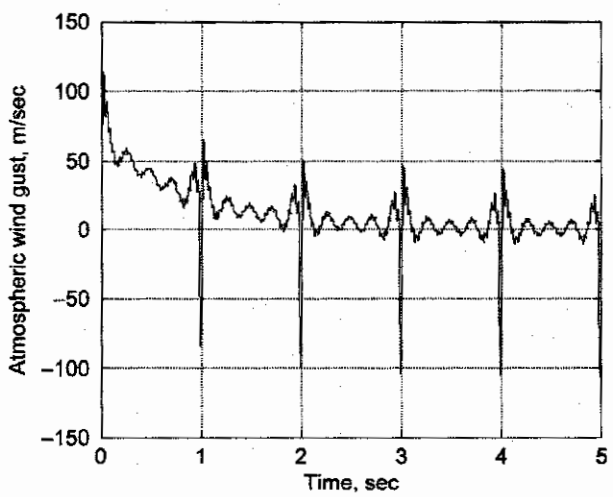

Figure 18.—Combined atmospheric wind gust for disturbance frequencies 5 to 30 Hz, with $\varepsilon = 1.7\times10^{-3}$.

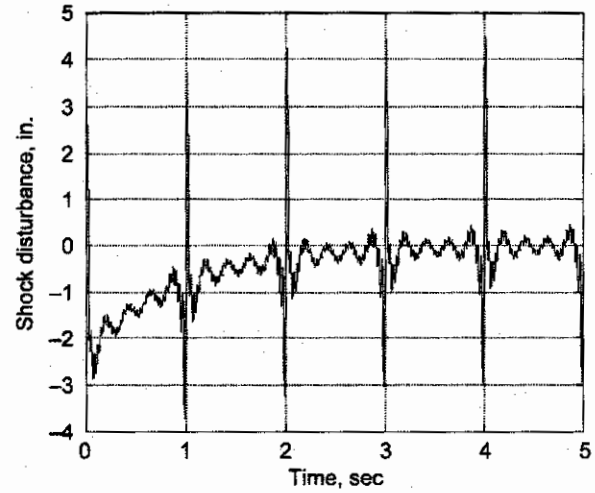

Figure 19.—Shock disturbance for disturbance frequencies 5 to 30 Hz, with $\varepsilon = 1.7\times10^{-3}$.

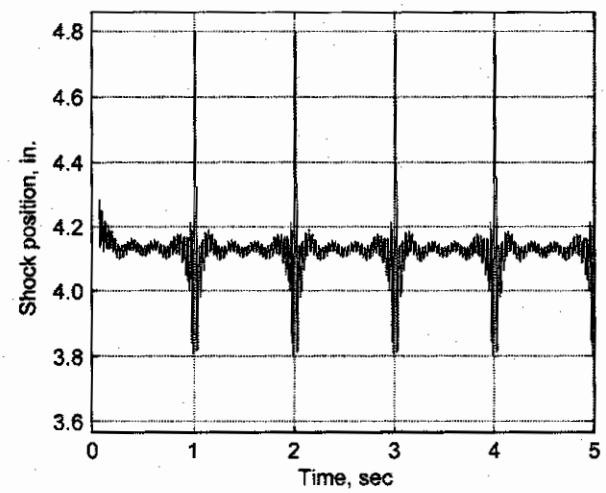

Figure 20.—Shock control response for disturbance frequencies 5 to 30 Hz, with $\varepsilon = 1.7\times10^{-3}$.

Based on the simulations carried out so far and with this control system design, it could be ascertained that the shock movement would be within about 0.4 in. peak-to-peak for light to moderate turbulence. For borderline severe turbulence [11] or for worst recorded turbulence [7], it could be ascertained that the controlled shock movement will be about 1 in. peak-to-peak. As it was discussed before, the value of ε is less at higher altitudes, thus, at supersonic flight altitudes it could be that an ε value in the order of 1×10^{-3} would be near the highest expected.

CONCLUSION

This paper describes an atmospheric turbulence model that has been developed to approximate the actual fractional nature of atmospheric turbulence. Also, this model has been scaled and extended to include temperature disturbances, wind gusts due to temperature, as well as pressure and density disturbances. Considerations for atmospheric turbulence specifications have been discussed for high speed atmospheric

Copyright © 2010 by ASME

vehicles, and a controls design example involving the shock positioning control design of a supersonic inlet are also described. The objective in this paper is to first, show how atmospheric disturbances are derived, and secondly, how to use these disturbances to potentially specify and design controls for high speed vehicles. As such, the emphasis is to demonstrate a design and analysis approach, and not to come up with an encompassing controls system design that considers all possible disturbances and operating scenarios. For the future, the attempt will be to come up with more detailed specifications for atmospheric disturbances and refine the analysis. Also, these studies will be extended to an integrated supersonic aero-propulso-servo-elastic vehicle system in order to study integrated vehicle stability and ride quality.

ACKNOWLEDGMENTS

The author would like to express his gratitude to the Supersonics Project of the NASA Fundamental Aeronautics Program for supporting this research effort.

REFERENCES

1. Nastrom, G. D.: Gage, K. S.; "A Climatology of Atmospheric Wavenumber Spectra of Wind and Temperature Observed by Commercial Aircraft," Journal of Atmospheric Sciences, vol. 42, No. 9, May 1985, pp. 950–960.
2. Fairall, C. W.: White, A. B.; Thompson, D. W.; "A Stochastic Model of Gravity-Wave-Induced Clear-Air Turbulence," Journal of Atmospheric Sciences, vol. 48, No. 15, August 1991.
3. Tatarski, V. I.: "Wave propagation in a Turbulent Medium," McGraw-Hill, 1961.
4. Kolmogorov, A. N.: "Dissipation of energy in the locally isotropic turbulence," Comptes rendus (Doklady) de l'Académie des Sciences de l'U.R.S.S., 32, 16–18, 1941.
5. Kolmogorov, A. N.: "The local structure of turbulence in incompressible viscous fluid for very large Reynold's numbers," Comptes rendus (Doklady) de l'Académie des Sciences de l'U.R.S.S., 30, 301–305.
6. Houbolt, J. C.: Steiner, R.; and Pratt, K. G.; 'Dynamic Response of Airplanes to Atmospheric Turbulence Including Flight Data on Input Response," NASA TR R–199, June 1964.
7. Tank, W. G.: "Atmospheric Disturbance Environmental Definition," NASA CR–195315, Feb. 1994.
8. Hoblit, F. M.: "Gust Loads on Aircraft: Concepts and Applications," AIAA Education Series, 1988.
9. Kopasakis, G.: "Atmospheric Turbulence Modeling for Aero Vehicles – Fractional Order Fits," NASA/TM to be published.
10. Tank, W. G.; Gillis, J.: "Atmospheric Disturbance Models for Linear and Nonlinear System Response Analysis," AIAA 34th Aerospace Sciences Meeting and Exhibit, Reno, NV, Jan. 1996.
11. McMinn, J. D.: Extension of a Kolmogorov Atmospheric Turbulence Model for Time-Based Simulation Implementation," AIAA Guidance Navigation and Control Conference, AIAA–97–3532, New Orleans, LA, August 11-13, 1997.
12. Johnson, D. L.; "Terrestrial Environment (Climatic) Criteria for Use in Aerospace Vehicle Development," 1993 Revision; NASA TM–4511, August 1993.
13. Soreide, D. C.: Tank, W. G.: "Proposed Model of the Atmosphere for the High Speed Civil Transport Program," to be Published.
14. Ashun, U.: Merchant, A.: Paduano, J.: Drela, M.: "Design of an Actively Stabilized, Near- Isentropic Supersonic Inlet," AIAA Computational Fluid Dynamics Conference, AIAA–2003–4069 Orlando, FL, 23-26 June 2003.
15. Tank, W. G.; Gillis, J.: "Atmospheric Disturbance Models for Linear and Nonlinear System Response Analysis," AIAA 34th Aerospace Sciences Meeting and Exhibit, Reno, NV, Jan. 1996.
16. Kopasakis, G.; Connolly, J W.: "Shock Positioning Controls Design for a Supersonic Inlet," AIAA 45th Joint Propulsion Conference, AIAA–2009–5117, Denver, CO, 2-5 August, 2009.
17. Kopasakis, G., "Feedback Control Systems Loop Shaping Design With Practical Considerations," NASA/TM—2007-215007, Sept. 2007.

Copyright © 2010 by ASME